Use of Ionic Liquids for π-Conjugated Polymer Electrochemical Devices

Wen Lu,[1] Andrei G. Fadeev,[1] Baohua Qi,[1] Elisabeth Smela,[1] Benjamin R. Mattes,[1]* Jie Ding,[2] Geoffrey M. Spinks,[2] Jakub Mazurkiewicz,[2] Dezhi Zhou,[2] Gordon G. Wallace,[2] Douglas R. MacFarlane,[3] Stewart A. Forsyth,[3] Maria Forsyth[3]

π-Conjugated polymers that are electrochemically cycled in ionic liquids have enhanced lifetimes without failure (up to 1 million cycles) and fast cycle switching speeds (100 ms). We report results for electrochemical mechanical actuators, electrochromic windows, and numeric displays made from three types of π-conjugated polymers: polyaniline, polypyrrole, and polythiophene. Experiments were performed under ambient conditions, yet the polymers showed negligible loss in electroactivity. These performance advantages were obtained by using environmentally stable, room-temperature ionic liquids composed of 1-butyl-3-methyl imidazolium cations together with anions such as tetrafluoroborate or hexafluorophosphate.

Dopable π-conjugated polymers such as polyaniline (PANI), polypyrrole (PPy), and polythiophene (PT) have attracted attention for application in various electrochemical devices including batteries, capacitors, electrochromic windows and displays, actuators, photovoltaic cells, and light-emitting electrochemical cells (*1*). While considerable effort has been expended toward the development of new high-performance π-conjugated polymer materials (*1*), less attention has been paid to the importance of the electrolyte in determining device performance. The realization of practical, long-lived π-conjugated polymer electrochemical devices therefore remains an elusive goal because of performance limitations that include poor environmental stability, slow switching speeds, and short lifetimes when electrochemically cycling between oxidation states. These problems derive partly from the electrolytes used in the devices, whether they are based on aqueous, organic, gel, or polymer electrolytes. Improved electrolytes are needed that simultaneously satisfy the requirements of high ionic conductivity ($>10^{-4}$ S cm^{-1}), large electrochemical windows (>1 V) over which the electrolyte is neither reduced nor oxidized at an electrode, fast ion mobility during redox events ($>10^{-14}$ m^2 V^{-1} s^{-1}), low volatility, and environmental stability. Certain members of the family of materials known as ionic liquids meet all of these requirements (*2*). We report on the utility of room-temperature ionic liquid electrolyte systems (ILES) for the synthesis, fabrication, and operation of π-conjugated polymer electrochemical mechanical actuators and high-performance electrochromic windows and numeric displays. It is important to note that no part of our work was performed in inert atmosphere glove boxes, which are often required for preparation and operation of π-conjugated polymer electrochemical devices.

Electrochemical actuators and electrochromic devices. The π-conjugated polymers are being studied worldwide (*3*–*7*) for electrochemical mechanical actuation because of properties that include light weight, high stress generation, large linear displacement (actuation strain), and low operational voltages. The mechanism for actuation is due primarily to the reversible transport of ions (*8*, *9*) and solvent molecules (*10*) between the polymer and the electrolyte during electrochemical oxidation and reduction. The resulting large dimensional changes generate stresses that exceed those of mammalian muscle (~0.1 to 0.5 MPa) by at least an order of magnitude with less than one volt driving voltage (*5*). Additionally, linear strains up to tenfold greater than piezoelectric polymers (typically <0.1%) are realized.

To date, most of the research on π-conjugated polymer actuators has been carried out in aqueous electrolytes; however, these systems suffer from narrow electrochemical potential windows and high volatility. These factors limit the lifetime and performance of a device. For example, electrochemical degradation of polyaniline occurs after only a few cycles in some aqueous electrolytes (*11*, *12*) because of nucleophilic attack on, and hydrolysis of, the polymer (*13*). Nonaqueous electrolytes, e.g., lithium salts in propylene carbonate (PC) can be used to improve the performance of polyaniline (*14*, *15*), and other π-conjugated polymer electrochemical actuators (*16*). PC has a relatively high boiling point (241.7°C), low vapor pressure (0.039 mm Hg), high dielectric constant (64.4), high ionic conductivity with dissolved lithium salts (0.1 to 1.0 mS/cm), and a relatively broad electrochemical window (–1.9 to + 1.7 V versus saturated calomel electrode). Nevertheless, organic electrolyte systems are still susceptible to evaporation, thus limiting the operational voltage range and device lifetime.

When π-conjugated polymers are electrochemically cycled in the presence of an electrolyte, their color changes; the absorption wavelength depends on the width of the polymer's bandgap. π-Conjugated polymers are being studied for electrochromic (EC) applications because of properties that include ease in the fabrication of large area, high-quality, optically transparent thin films, excellent coloration contrast and matching, rapid coloration rates, and low operational voltages (*1*). EC windowpane glass holds promise for the thermal management of buildings, while EC displays are promising competitors for liquid crystal display technologies. The mechanism for the color change in π-conjugated polymers, as well as device performance limitations with respect to stability and lifetimes, are analogous to those discussed above for electrochemical mechanical actuators.

Ionic liquids. Ionic liquids (IL) are not new; for example, ethyl ammonium nitrate ($[EtNH_3][NO_3]$), which has a melting point of 12°C, was first described in 1914 (*17*). Typically, ionic liquids consist of nitrogen-containing organic cations and inorganic anions. As they are nonvolatile and nonflammable, have high thermal stability, and are relatively inexpensive to manufacture, ionic liquids are now finding applications in chemical synthesis, catalysis, separation technology, and the fabrication of conventional electrochemical devices (*18*).

Ionic liquids are salts that are fluid over a wide temperature range, including room temperature, with higher viscosities (10^{-2} to 10^0 Pa s) than either aqueous ($<10^{-3}$ Pa s) or organic ($\sim 6 \times 10^{-3}$ Pa s) electrolytes at room temperature. When compared with other electrolytes, some ionic liquids also have the advantage that they can be obtained in a very dry state, making them especially suitable for applications in electrochemical systems from which moisture must be excluded over long periods of operation. Furthermore, some ionic liquid relatives are plastic solids at room temperature yet still maintain reasonable conductivity (*19*), and others can be transformed into soft, elastomeric solids at room temperature by the addition of small amounts (~5%) of a suitable polymer (*20*).

[1]Santa Fe Science and Technology (SFST), 3216 Richards Lane, Santa Fe, NM 87507, USA. [2]Intelligent Polymer Research Institute (IPRI), University of Wollongong, NSW, Australia. [3]Monash University, Department of Chemistry, Victoria, Australia.

*To whom correspondence should be addressed. E-mail: mattes@sfst.net

Despite being reported in a variety of electrochemical devices (*21*–*25*), investigation of ionic liquids for π-conjugated polymer electrochemistry is limited. Osteryoung *et al*. prepared PANI in $AlCl_3$-1-ethyl-3-methyl imidazolium chloride ionic liquids and studied its electrochemistry in this environmentally unstable ILES (*26*, *27*). As the anion of this electrolyte system is highly reactive on exposure to moisture in air, it is not broadly useful for electrochemical devices.

We present results on the synthesis, fabrication, and operation of π-conjugated polymer devices in environmentally stable ionic liquids composed of 1-butyl-3-methyl imidazolium cation ($BMIM^+$) and either the tetrafluoroborate (BF_4^-) or hexafluorophosphate (PF_6^-) anions. Both of these ionic liquids possess negligible vapor pressures, high ionic conductivities (1 to 5 mS/cm), and broad electrochemical windows (–2.5 to +2.5 V versus Ag/Ag^+). All electrochemical results herein are referenced to the Ag/Ag^+ electrode.

Actuation properties of polyaniline fiber with ionic liquids. A 10-mm length of 59 μm diameter wet-spun polyaniline emeraldine base (EB) fiber was fully doped with trifluoromethanesulfonic (triflic) acid (*28*) according to the scheme in Fig. 1A. The dry Panion triflate fiber (fig. S1) had, in air, a Young's elastic modulus of 3 GPa, ultimate tensile strength of 200 MPa, and an elongation at break of 15%. Because the fiber had a high conductivity (300 S/cm), it did not need to be coated with metal to achieve uniform charge distribution throughout its length.

The electrochemical mechanical linear actuation performance for the leucoemeraldine/emeraldine salt (LE/ES) redox couple (Fig. 1B) in $[BMIM][BF_4]$ was measured according to (*28*). Fig. 2A shows that the isotonic strain (ΔL/L with constant applied force of 0.0098 N) measured during one cyclic voltametric (CV) redox cycle reached a maximum value of 0.28%, while the isometric stress (generated force normalized to the fiber's cross-sectional area, Fig. 2B) was 1.8 MPa. These values are nearly identical to those cited by Mazzoldi *et al*. (*14*) for a PANI fiber in aqueous and gel electrolytes. The strain was contractile when the polymer was oxidized from the fully reduced leucoemeraldine (–0.4 V) state to the emeraldine salt (+0.8V) state, and expansive upon reduction, indicating that cation incorporation at negative potentials and expulsion at positive potentials is the predominant strain-generating mechanism during actuation (Fig. 1B).

The ratio of the mass lifted to the mass of fiber was $\sim 2 \times 10^4$. Energy efficiencies were low (~0.01%) owing to polymer and electrolyte resistive losses. The energy density (volumetric work capacity) for one cycle was 10 kJ/m^3 (the same as mammalian muscle), and the specific work performed was 5.6 J/kg. The power/volume ratio was 42 W/m^3 with a specific power of 0.023 W/kg. These power values are low because of the extremely low frequencies used for the CV scan (0.0042 Hz). For many types of actuator materials, it is known that power is proportional to the frequency of stimulation (*29*). The measured strain rates were also low (0.012% s^{-1}) for the same reasons. Faster movement may be achieved by using thinner fibers of higher conductivity and/or faster pulses with greater potential drive windows (*30*), as demonstrated below, with either approach enhancing the diffusion of ions into and out of the polymer.

We were able to correlate the amount of injected and removed charge during the oxidation and reduction cycle with the electrochemically produced strain and stress (Fig. 2, C and D). The charge during a square wave potential pulse between –0.4 to 0.7 V over one 70-s period (*31*) was determined by integrating the measured current with respect to the time of the period. The strain and stress responses with respect to charge are shown in Fig. 2E. The electrochemically induced actuation of the fiber is linearly proportional to the amount of injected or removed charge, as has been found previously for standard electrolytes (*32*). We calculate a strain to charge ratio of –0.031% mC^{-1}, the negative sign indicating the fiber's contraction during its oxidation, and a stress to charge ratio of 0.18 MPa mC^{-1}. By plotting the linear portions of the charge and discharge versus time curves (Fig. 2, C and D), we determined the charging rate to be 0.40 mC s^{-1} and the discharge rate to be –0.63 mC s^{-1}. The absolute value of the discharging rate is greater than that of the charging rate, indicating that the kinetics for the polymer's reduction are faster than for the oxidation in $[BMIM][BF_4]$.

In lifetime tests of the fiber, both electroactivity and electromechanical actuation continued without significant decrease (< 1%) in either stress or strain for 10,000 redox cycles, after which the test was stopped. This unprecedented level of performance shows the clear benefit of ILES for π-conjugated polymer electrochemical actuator devices. Unlike aqueous electrolyte systems, the redox mechanism in $[BMIM][BF_4]$ does not involve the loss or gain of solvated protons, and we observe no pH dependence toward electroac-

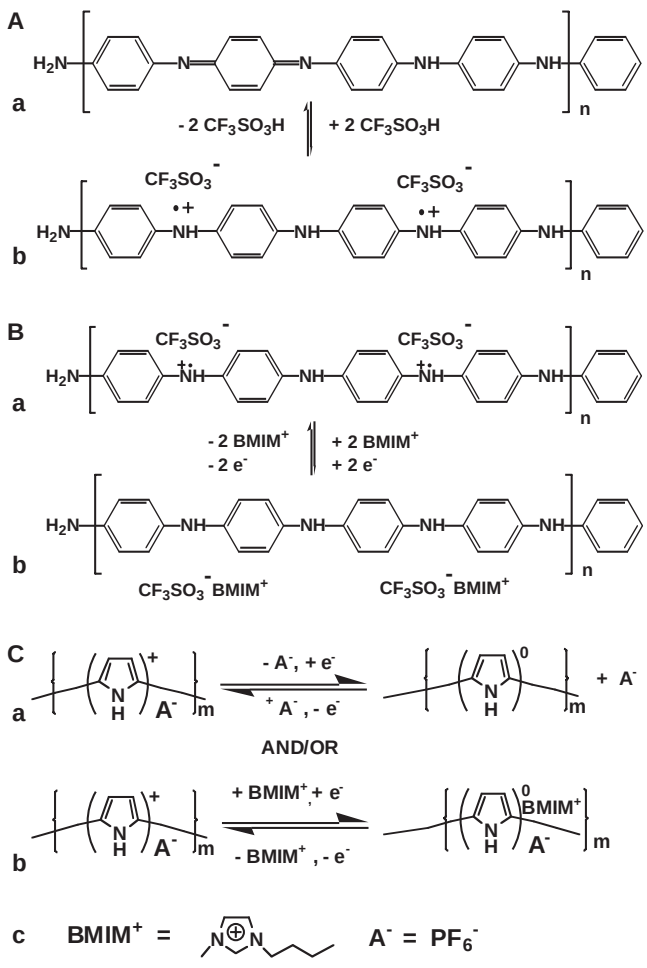

Fig. 1. (**A**) When polyaniline in the nonconductive emeraldine base (EB) oxidation state (a) is immersed in an acid-like trifluoromethanesulfonic acid (CF_3SO_3H), a highly conductive radical cation (separated polaron) structure forms (b), which is known as emeraldine salt (ES). This does not involve any change in the electrochemical potential of the polymer. (**B**) ES (a) is electrochemically reduced to the leucoemeraldine (LE) structure (b) by gaining two electrons per tetrameric repeat unit at low potentials (~–0.4 V versus Ag/Ag^+). LE loses two electrons in pH-neutral $[BMIM][BF_4]$ to directly form the ES structure when it is cycled to higher positive potentials (+0.8 V versus Ag/Ag^+). Since it is improbable that protons are exchanged in this mechanism, oxidation of LE to ES, and the reduction of ES to LE, can only be explained by the direct loss/gain of electrons and $BMIM^+$ cation intercalation/de-intercalation. The cation from the ILES serves the role of maintaining overall electro-neutrality of the polymer during charging/discharging. (**C**) Oxidation and reduction of PPy-PF_6 in $[BMIM][PF_6]$ may involve either the de-intercalation/intercalation of the PF_6^- anion at high potentials (a), and/or the intercalation/de-intercalation of the $BMIM^+$ cation at low potentials (b). The structure of the $BMIM^+$ cation and the PF_6^- anion are given in (c).

tivity or actuation in pH neutral ionic liquids for our polyaniline fiber.

Polyaniline and polypyrrole actuator devices with ionic liquids. In order to demonstrate the applicability of the above results to devices, we next fabricated two π-conjugated polymer actuator systems based on both wet-spun polyaniline fiber configured as a yarn and electrochemically synthesized polypyrrole tubes grown on top of helical Pt metal wire substrates. First, a 10-mm length of a twisted 20-strand yarn (three turns cm^{-1}) was prepared from Panion triflate monofilament fibers (fig. S1). An enhanced linear displacement of 0.8% was determined for the yarn in [BMIM][BF_4] compared with 0.28% strain for an individual fiber. The maximum force generated for the 20-fiber twisted yarn was 0.028 N, compared with 0.005 N for a single fiber. These measurements were made by cycling the yarn at a rate of 5 mV s^{-1} between −0.6 V and +1.2 V. It is likely that the increased strain and stress observed for the yarn compared with the individual fiber are due to the increased charge injection obtained by cycling to higher potentials.

The yarn provides a technologically practical packaging method for constructing long-lived environmentally stable electrochemical mechanical actuators at the macroscopic scale. This method enables us to increase the electroactive surface area of the device, and further improvement in performance is anticipated with the next generation of fiber produced with smaller diameters (10 to 30 μm), which will enable faster rates of ion diffusion.

A second electrochemical mechanical actuator was constructed from a polypyrrole (PPy-PF_6) hollow tube with a spiral-wound Pt wire interconnect that was integrated into the inner wall of the device as a means of providing efficient charge distribution and torsional rigidity (fig. S2). Initially, the electrochemistry of the PPy-PF_6 to be used as the actuating material was investigated using a thin film of PPy-PF_6 electrodeposited onto a platinum disc electrode (Fig. 3A). Tetrabutylammonium hexafluorophosphate (TBAPF_6) in propylene carbonate and pure [BMIM][PF_6] were used as the supporting electrolyte. The magnitude of the current flow observed during CV scans showed that the oxidation and reduction processes were comparable in [BMIM][PF_6] and in PC-TBAPF_6 electrolytes. The appearance of an additional peak at more positive potentials in [BMIM][PF_6], suggests that more complex, largely irreversible electrochemical processes occur in this system at high potentials.

As in the case of the polyaniline fiber, the PPy-PF_6 strain and electroactivity in the ILES were stable over several thousand scans, indicating that little, if any, polymer degradation occurred. Using the two-electrode actuator set-up shown in (fig. S3), a symmetric square wave potential pulse (±5V, 1 Hz) was applied to the PPy-PF_6 actuator in either PC containing 0.25 M TBAPF_6 or pure [BMIM][PF_6] electrolyte. The displacement under a 0.049 N load and the normalized redox charge, i.e., the charge as a fraction of the charge exchanged during the 100th cycle, were monitored as a function of the number of potential pulse cycles (Fig. 3B). The normalized redox charge can be used as a measure of the extent of change or degradation in the electrochemical properties of the actuator during prolonged cycling.

To compare the linear displacement, displacement rate, and electroactivity in the two electrolytes, the PPy-PF_6 actuator was cycled 6000 times. For a few hundred cycles, the linear displacement and the displacement rate were similar in both electrolytes. However, as Fig. 3B illustrates, the normalized charge ratio and the displacement decreased dramatically in PC-TBAPF_6 after 2000 cycles, but were markedly more stable in [BMIM][PF_6^-]. The decrease in performance observed in PC-TBAPF_6 can be attributed to breakdown of the polymer backbone (mechanical and electronic) that occurs in this electrolyte system, presumably because of nucleophilic attack on PPy-PF_6 as observed by others (*33*, *34*) at extreme potentials (*35*), and/or the electrochemical decomposition of PC, which has a narrower potential window. After 6000 cycles in [BMIM][PF_6], the observed displacement decreased by 17% (1.2 to 1.0%). However, after a "resting period" when the electrical stimulus was removed by switching the cell off for 1 hour (open circuit), the performance nearly reverted to the original levels, indicating that little irreversible degradation of the polymer had occurred. In the course of our studies, the best performance obtained for these two-electrode devices was 1.6% strain at a 3.2% s^{-1} rate of displacement, which is the same as the fastest polypyrrole actuators to date (*30*).

The direction of linear displacement for the device observed in [BMIM][PF_6] was opposite to that observed in PC-TBAPF_6. The application of a negative potential in PC-TBAPF_6 re-

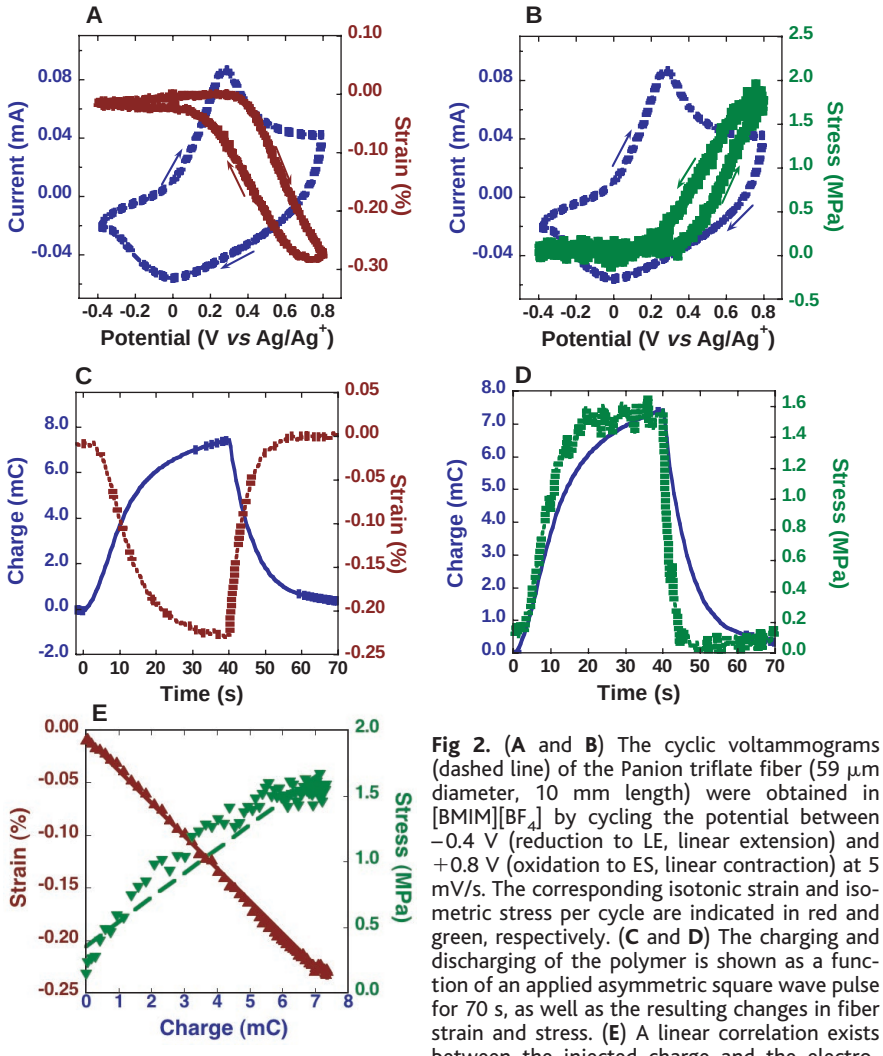

Fig 2. (**A** and **B**) The cyclic voltammograms (dashed line) of the Panion triflate fiber (59 μm diameter, 10 mm length) were obtained in [BMIM][BF_4] by cycling the potential between −0.4 V (reduction to LE, linear extension) and +0.8 V (oxidation to ES, linear contraction) at 5 mV/s. The corresponding isotonic strain and isometric stress per cycle are indicated in red and green, respectively. (**C** and **D**) The charging and discharging of the polymer is shown as a function of an applied asymmetric square wave pulse for 70 s, as well as the resulting changes in fiber strain and stress. (**E**) A linear correlation exists between the injected charge and the electrochemically induced strain (red point-up triangles), while the stress (green point-down triangles) is strongly correlated with the charge.

sulted in expulsion of PF_6^- ions and a decrease in volume (contraction), whereas in the same potential range in [BMIM][PF_6], expansion was observed, presumably owing to the incorporation of the large imidazolium cation (Fig. 1C). Interestingly, cation movement also predominated in the polyaniline actuators operated in ILES containing the imidazolium cation.

Electrochromic devices with ionic liquids. We next discuss our work on EC windows and numeric displays as further examples of π-conjugated polymer electrochemical devices that exhibit enhanced performance in ILES. Thin films of poly (3,4-ethylenedioxythiophene) tetrafluoroborate (PEDOT-BF_4^-), PANI-BF_4^-/$CF_3CO_2^-$, and PPy-BF_4^-, were electrochemically synthesized in [BMIM][BF_4] from their respective monomers (fig. S4). In comparison with the PPy-PF_6^- prepared in PC, the PPy-BF_4^- synthesized in [BMIM][BF_4] did not show an additional peak (fig. S4) at higher positive scanning potentials (*28*), which suggests that synthesis of π-conjugated polymers in ionic liquids may confer different materials properties. Electrochromic devices utilizing the first two of these films were constructed.

The exceptional stability of an electrochemically synthesized polyaniline electrochromic window is demonstrated in Fig. 4A; it showed no appreciable decrease in current flow after potential pulsing in [BMIM][BF_4], between −0.6 to 1.1 V at 1 Hz for 1,000,000 cycles, when the test was stopped [movie S1 (*28*)]. The highest number of cycles previously achieved for a π-conjugated polymer EC window at failure was reported to be 1 to 3 × 10^5 cycles (*36*).

The π-conjugated polymer EC numeric displays were constructed in a very simple manner (*28*). Either chemically synthesized polymer (via spin-coating) or electrochemically synthesized (from ionic liquids) thin films were patterned on ITO electrode substrates. PANI was employed as the anodically coloring polymer, while substituted polythiophenes [PEDOT and/or regioregular poly (3-octylthiophene) (POT)] were utilized as the cathodically coloring polymer (fig. S5). The operation of a 7-pixel numeric display is shown in movie S2 and its design in fig. S6. The maximum color contrast for the device was 35%, which is slightly greater than that of a similar EC device reported in (*37*). To improve the color contrast for the device, we used a composite polymer PEDOT-POT transparent thin film (obtained by electrochemically polymerizing PEDOT from [BMIM][BF_4] over a thin film of POT that was first spin-coated onto the ITO/glass electrode) as the cathodically coloring polymer material. This composite polymer structure can electrochemically drive PANI to higher oxidation states, i.e., from LE to ES, and then further into the higher pernigraniline oxidation state (*15*), which gives higher color contrast for the device. Well-defined cyclic voltammograms were obtained for the individual pixels of the PANI/[BMIM][BF_4]/PEDOT-POT numeric display (fig. S7). Low voltage was needed to drive the device. The UV-Vis-NIR spectra of an individual pixel in the bleached (–1.5 V) and colored (+1.5 V) states are shown in Fig. 4B. The transmitted light difference between the bleached and colored states was 63% at 560 nm, which satisfies requirements for a good display (*38*).

Figure 4C reveals the stable in situ transmittance change at 560 nm for an individual pixel upon voltage pulsing between –1.5 V and +1.5

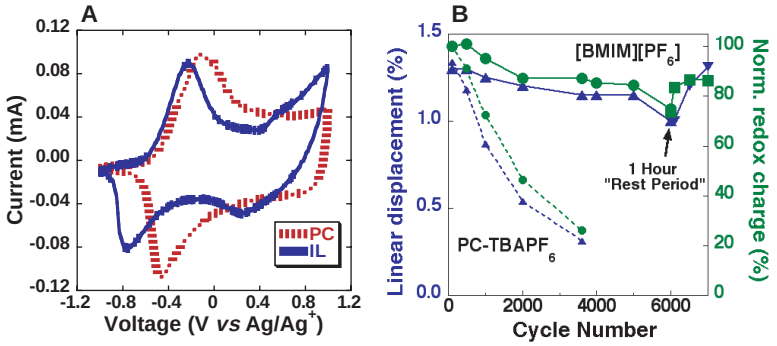

Fig. 3. (**A**) The cyclic voltammograms of two PPy-PF_6–coated platinum disk electrodes measured in either PC-$TBAPF_6$ or [BMIM][PF_6] at a scan rate of 100 mV s–1. The PPy-PF_6 thin-films were prepared galvanostatically, at one mA cm^{-2} for 3 min, using a solution containing 0.06 M PPy, 0.05 M $TBAPF_6$, and 1% water in propylene carbonate. (**B**) The strain (triangles) and normalized redox charge (circles and squares) performance for the PPy-PF_6 tube actuators grown onto a helical platinum wire were evaluated in either PC-$TBAPF_6$ or [BMIM][PF_6]. A potential pulse of +5 or –5 V (two-electrode cell) at 1 Hz was used. Note that after 6000 cycles the cell was switched off for 1 hour, and then electrical stimulation recommenced.

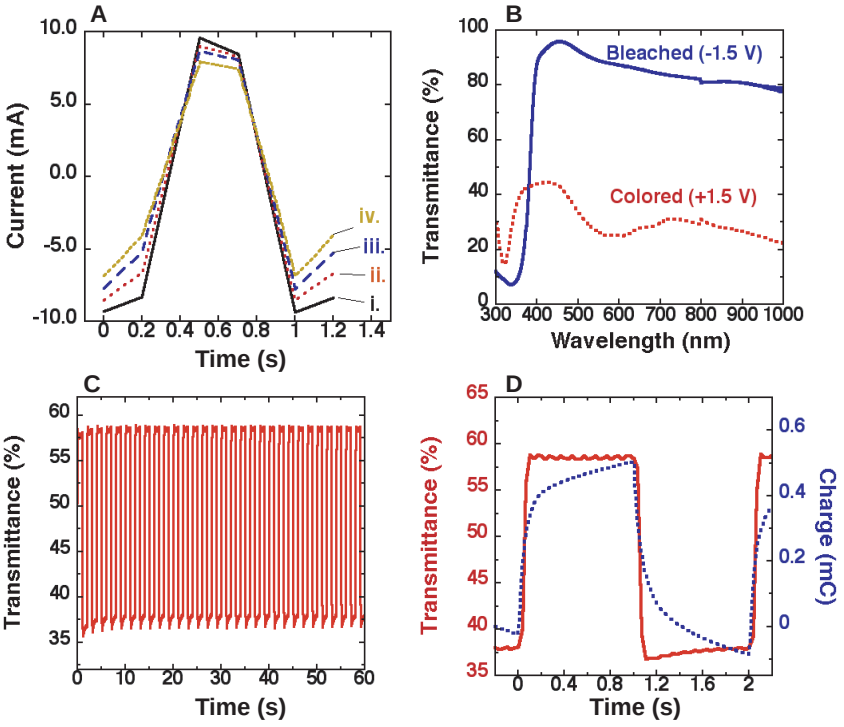

Fig. 4. (**A**) Current versus time curves during oxidation taken at various cycles in [BMIM][BF_4] for a polyaniline electrochromic window. Potential pulsing was performed between −0.6V and +1.1V (versus Ag/Ag^+) with a pulse width of 0.5 s: (i) the 3rd cycle, (ii) the 330,000th cycle, (iii) the 630,000th cycle, and (iv) the 1,000,000th cycle. (**B**) The UV-Vis-NIR spectra obtained for a pixel of a PANI/[BMIM][BF_4]/PEDOT-POT numeric display in the bleached (–1.5 V) and colored (+1.5 V) states. (**C**) The transmittance change (ΔT) obtained at 560 nm for a pixel of the same numeric display upon voltage switching between –1.5 V and +1.5 V with the pulse width of 1 s. (**D**) The charge versus time (dashed line) and ΔT versus time (solid line) curves for a display pixel upon voltage switching between –1.5 and 1.5 V with a pulse width of 1 s.

V during 1 min of operation. The current versus time curve showed a rapidly decaying current upon voltage switching, indicating the fast nature of the redox process for the device. Fig. 4D reveals that the total change in transmission from the bleached to the colored state consumed 0.5 mC of charge in 1 s. Within the first 100 ms, there was a fast coloration change with a 21% increase in transmittance, and 68% of total charge was consumed (as compared with the charge consumed after 1 s). This speed is comparable to good inorganic-based EC displays (*39*).

Conclusions. Our findings are significant for the area of electrochemical devices based on π-conjugated polymers because they can lead to long periods of stable device performance. This phenomenon was demonstrated for polyaniline fiber and yarn actuators, polypyrrole tube actuators, and for simple π-conjugated polymer electrochromic windows and numeric displays. The use of environmentally stable, room-temperature ionic liquids as electrolyte systems should have an impact on many areas of application in π-conjugated polymer electrochemical devices. Furthermore, as demonstrated herein for different π-conjugated polymer thin films, improved synthesis from ionic liquids may have positive effects on both their structure and properties.

References and Notes

1. T. A. Skotheim, R. L. Elsenbaumer, J. R. Reynolds, Eds., *Handbook of Conducting Polymers* (Dekker, New York, 1998).
2. W. Lu, B. R. Mattes, A. G. Fadeev, U.S. and PCT Patent Applications, filed on 21 December 2001.
3. W. Takashima, M. Kaneko, K. Kaneto, A. G. MacDiarmid, *Synth. Met.* **71**, 2265 (1995).
4. E. Smela, O. Inganäs, I. Lundström, *Science* **268**, 1735 (1995).
5. R. H. Baughman, *Synth. Met.* **78**, 339 (1996).
6. T. W. Lewis, S. E. Moulton, G. M. Spinks, G. G. Wallace, *Synth. Met.* **85**, 1419 (1997).
7. A. Della Santa, D. De Rossi, A. Mazzoldi, *Synth. Met.* **90**, 93 (1997).
8. Q. Pei, O. Inganäs, *Sol. State Ion.* **60**, 161 (1993).
9. M. R. Gandhi, P. Murray, G. M. Spinks, G. G. Wallace, *Synth. Met.* **73**, 247 (1995).
10. L. Bay, T. Jacobsen, S. Skaarup, K. West, *J. Phys. Chem. B* **105** (36), 8492 (2001).
11. T. Kobayashi, H. Yoneyama, H. Tamura, *J. Electroanal. Chem.* **161** (1984).
12. E. M. Genies, C. Tsintavis, *J. Electroanal. Chem.* **200**, 127 (1986).
13. Y. Li, R. Qian, *Synth. Met.* **53**, 149 (1993).
14. A. Mazzoldi, C. Degl'Innocenti, M. Michelucci, D. De Rossi, *Mater. Sci. Eng.* **C6**, 65 (1998).
15. W. Lu, B. R. Mattes, in preparation
16. T. W. Lewis, G. M. Spinks, G. G. Wallace, D. De Rossi, M. Pachetti, *Polym. Prep.* **38**, 520 (1997).
17. P. Walden, *Bull. Acad. Imper. Sci.* (St. Petersburg), 1800 (1914).
18. M. Freemantle, *Chem. Eng. News*. **78**, 37 (2000).
19. D. R. MacFarlane, M. Forsyth, *Adv. Mater.* **13**, 957 (2001).
20. C. Tiyapiboonchaiya, D. R. MacFarlane, J. Sun, M. Forsyth, *Macromol. Chem. Phys.*, in press.
21. V. R. Koch, C. Nanjundiah, G. B. Appetecchi, B. Scrosati, *J. Electrochem. Soc.* **142**, L116 (1995).
22. J. S. Wilkes, M. J. Zaworotko, *Chem. Commun.* **1992**, 965 (1992).
23. R. T. Carlin, H. C. D. Long, J. Fuller, P. C. Trulove, *J. Electrochem. Soc.* **141**, L73 (1994).
24. P. Bonhôte, A.-P. Dias, N. Papageorgiou, K. Kalyanasundaram, M. Grätzel, *Inorg. Chem.* **35**, 1168 (1996).
25. N. Papageorgiou *et al*., *J. Electrochem. Soc.* **143**, 3099 (1996).
26. J. Tang, R. A. Osteryoung, *Synth. Met.* **45**, 1 (1991).
27. _____, *Synth. Met.* **44**, 307 (1991).
28. Materials and methods are available as supporting material at *Science* Online.
29. J. E. Huber, N. A. Fleck, M. F. Ashby, *Proc. R. Soc. Lond. A* **453**, 2185 (1997).
30. J. D. Madden, R. A. Cush, T. S. Kanigan, I. W. Hunter, *Synth. Met.* **113**, 185 (2000).
31. An asymmetric square wave pulse (40 s for oxidation and 30 s for reduction) allows the fiber to achieve steady states of actuation and balanced motion in the experiment.
32. T. F. Otero, J. M. Sansiñena, *Bioelectrochem. Bioenerg.* **42**, 117 (1997).
33. J. B. Schlenoff, H. Xu, *J. Electrochem. Soc.* **9**, 2397 (1992).
34. F. Beck, U. Barsch, R. Michaelis, *J. Electroanal. Chem.* **351**, 169 (1993).
35. It has come to our attention since acceptance of this paper that cycling [BMIM][PF_6] at potentials beyond its electrochemical window may lead to decomposition products that form an explosive mix. Caution from the authors is thus advised in selecting appropriate potential limits.
36. P. Chandrasekhar *et al*., *Adv. Funct. Mater.* **12**, 95 (2002).
37. D. DeLongchamp, P. T. Hammond, *Adv. Mater.* **13**, 1455 (2001).
38. S. A. Sapp, G. A. Sotzing, J. R. Reynolds, *Chem. Mater.* **10**, 2101 (1998).
39. M. Gratzel, *Nature* **409**, 575 (2001).

40. The polyaniline fiber actuator and the electrochromic devices in [BMIM][BF_4] material are based on work supported by the Defense Advanced Research Projects Agency Defense Sciences Office for which the Santa Fe authors are thankful. The Australian Research Council and Quantum Technology of Sydney supported the polypyrrole tube in [BMIM][PF_6] actuator work for which the Wollongong and Monash University contributors are grateful.

Supporting Online Material

www.sciencemag.org/cgi/content/full/1072651/DC1
Materials and Methods
Figs. S1 to S7
Movies S1 and S2

8 April 2002; accepted 20 June 2002
Published online 4 July 2002;
10.1126/science.1072651
Include this information when citing this paper.

Brownian Motion of DNA Confined Within a Two-Dimensional Array

Dmytro Nykypanchuk, Helmut H. Strey,* David A. Hoagland*

Linear DNA molecules are visualized while undergoing Brownian motion inside media patterned with molecular-sized spatial constraints. The media, prepared by colloidal templating, trap the macromolecules within a two-dimensional array of spherical cavities interconnected by circular holes. Across a broad DNA size range, diffusion does not proceed by the familiar mechanisms of reptation or sieving. Rather, because of their inherent flexibility, DNA molecules strongly localize in cavities and only sporadically "jump" through holes. Jumping closely follows Poisson statistics. By reducing DNA's configurational freedom, the holes act as molecular weight–dependent entropic barriers. Sterically constrained macromolecular diffusion underlies many separation methods and assumes an important role in intracellular and extracellular transport.

Under incessant Brownian motion, mobile macromolecules in gels, membranes, or cytoplasm constantly squeeze through and around molecular-size obstructions. Until recently, neither the surroundings nor the motion of a single molecule could be directly observed, and the understanding of such sterically constrained motions was principally deduced through examination of the macroscopic diffusion coefficient. The dynamics of a single, large macromolecule can now be visually monitored by fluorescence microscopy (*1*–*4*), but studies of macromolecular diffusion by this approach have not extended to environments providing well-defined spatial constraints. We describe how to prepare highly ordered media in which macromolecular motion can be observed. Our preparation method, colloidal templating, provides regular microporous arrays of controlled geometry and chemistry.

Three basic mechanisms have emerged to explain how flexible macromolecules diffuse within a constraining medium—sieving, en-

Department of Polymer Science and Engineering, University of Massachusetts Amherst, Amherst, MA 01003, USA.

*To whom correspondence should be addressed. E-mail: strey@mail.pse.umass.edu (H.H.S.) and dah@neurotica.pse.umass.edu (D.A.H.).